Operational experience with the CMS pixel detector in LHC Run II

To cite this article: J. Karancsi 2016 *JINST* **11** C12057

Published by IOP Publishing for Sissa Medialab

Received: *October 28, 2016*
Accepted: *December 13, 2016*
Published: *December 21, 2016*

Pixel 2016 International Workshop
September 5 – September 9, 2016
Sestri Levante, Genova, Italy

2016 JINST 11 C12057

Operational experience with the CMS pixel detector in LHC Run II

J. Karancsi[1] **on behalf of the CMS collaboration**

Institute for Nuclear Research, Hungarian Academy of Sciences,
Bem ter 18/c, Debrecen, 4026 Hungary
Institute of Experimental Physics, University of Debrecen,
Bem ter 18/a, Debrecen, 4026 Hungary
CERN,
Route de Meyrin, Geneve 23, CH-1211 Switzerland

E-mail: janos.karancsi@cern.ch

Abstract: The CMS pixel detector was repaired successfully, calibrated and commissioned for the second run of Large Hadron Collider during the first long shutdown between 2013 and 2015. The replaced pixel modules were calibrated separately and show the expected behavior of an un-irradiated detector. In 2015, the system performed very well with an even improved spatial resolution compared to 2012. During this time, the operational team faced various challenges including the loss of a sector in one half shell which was only partially recovered. In 2016, the detector is expected to withstand instantaneous luminosities beyond the design limits and will need a combined effort of both online and offline teams in order to provide the high quality data that is required to reach the physics goals of CMS. We present the operational experience gained during the second run of the LHC and show the latest performance results of the CMS pixel detector.

Keywords: Detector alignment and calibration methods (lasers, sources, particle-beams); Performance of High Energy Physics Detectors; Pixelated detectors and associated VLSI electronics

[1]Supported by the Hungarian Scientific Research Fund under contract number OTKA K 109803.

doi:10.1088/1748-0221/11/12/C12057

Contents

2016 JINST 11 C12057

1 Introduction

The pixel detector, which is the innermost part of the CMS Silicon tracker system [1], consists of three cylindrical barrel layers at 4 cm, 7 cm and 11 cm distance from the beam pipe, and two endcap disks on each side. It has more than 65 million pixels, each with a size of 100 μm $\times$ 150 μm. The detector has been repaired, recommissioned and calibrated during the first long shutdown of the LHC (LS1) in preparation for the second data-taking period (Run II) [2]. Most of the faulty components were successfully repaired or replaced with spare or new modules. The operational temperature was decreased from 0°C to −10°C. Most of the calibrations were carried out before the first collisions took place. The performance of the detector was evaluated using collision events. The timing and the bias voltage were adjusted to achieve the best hit efficiency and resolution. Throughout Run II, the detector performance was strictly monitored in order to assure the best possible performance. In 2016, the detector was operating at instantaneous luminosities that surpassed its design capabilities with an overall good performance. It is scheduled to be replaced with the new Phase I detector [3], which exceeds the current detector limitations.

2 Run II Start-up operations

2.1 Calibrations

The initial commissioning of the detector before the first collisions comprised a series of routine procedures [4]. These include the analog signal offset (baseline) adjustments of the optical receivers

in the front end and the analog address level calibration of pixels. In order to cope with the enormous data rate, the detector features analog zero-suppressed readout, which means that pixels with accumulated charges below a certain threshold are discarded. Thresholds are minimized in an iterative way to maintain high efficiency. The calibrations further include pulse height optimization and optical conversion adjustments. Then the timing of the readout is measured and tuned during the first collisions (figure 1) in a fine delay scan where the best setting is determined by simultaneously maximizing hit — and charge collection efficiency.

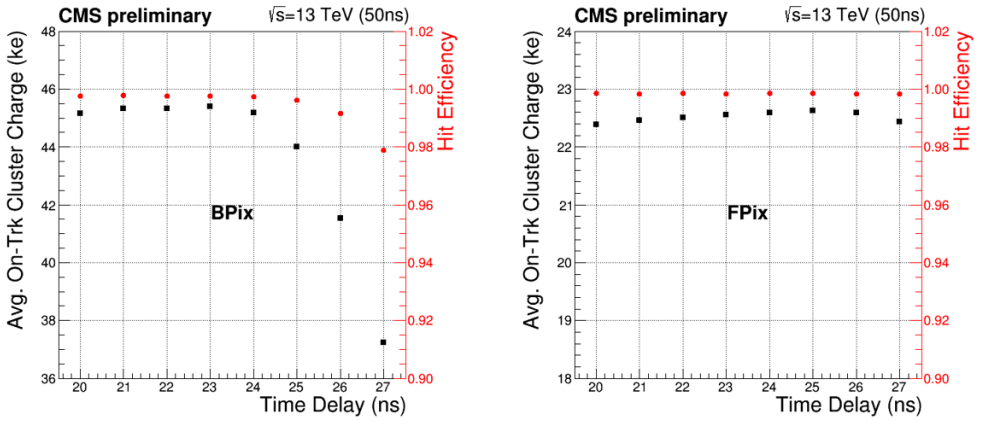

Figure 1. Average charge for clusters on track (black, left axis) and hit efficiency (red, right axis) vs. time delay setting for a) barrel and b) forward modules. The charge is not corrected for the path of the incoming particle in the silicon. The current time delay setting is 22 ns.

2.2 Good detector fraction

All modules were repaired during LS1, but in the commissioning eight modules showed faulty behavior (figure 2). In addition, during the operation in nominal magnetic field of 3.8 T, a sector (a power and a read-out group) in a half-shell of the barrel signaled an under-voltage problem (figure 2b). There was no solution found to recover all modules but a stable configuration was found that allowed to keep layer 1 and 3 modules functional. The good detector fraction during stable operation is 98.3% for the barrel and 99.98% for the forward pixels where only a single readout chip (ROC) is not operational (figure 3).

2.3 High voltage bias scan

In order to achieve a better resolution, the high voltage bias of the barrel modules was increased from 150 V to 200 V. During first collisions, a high voltage scan [5] was carried out, and the cluster properties and hit efficiency were measured to validate the new setting (figure 4), which is expected to remain optimal throughout the year.

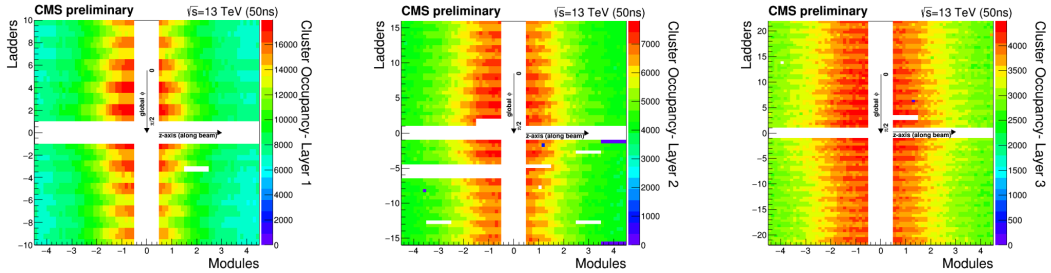

(a) **(b)** **(c)**

Figure 2. Cluster occupancy as a function of ladders (along global ϕ) and modules (along the beam axis) for a) layer 1, b) layer 2 and c) layer 3 readout chips. The middle cross-shaped areas are invalid coordinates, while other white areas show readout chips with zero occupancy.

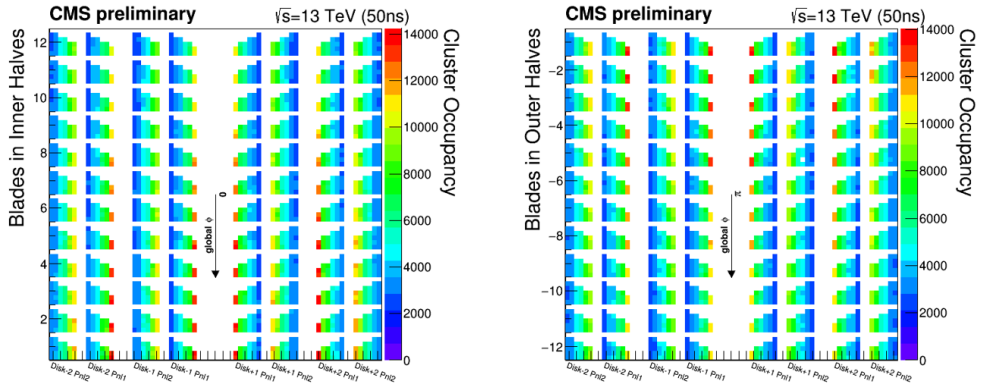

(a) **(b)**

Figure 3. Cluster occupancy as a function of blades (along global ϕ) and forward disks (along the beam axis) for readout chips facing a) towards and b) away from the center of the LHC. Two triangle-like panels, sandwiched together facing the opposite direction, form a single blade with modules of increasing length with radii. The panels are drawn in two separate columns for each disk.

3 Performance measurements during stable running

3.1 Lorentz angle

In CMS the magnetic field is parallel to the beam which causes the charge carriers to drift within the pixel sensors. This in turn creates larger clusters, which allow an improved position estimate and better resolution. For barrel layer modules the direction of the Lorentz drift is perpendicular to the beam. For them, the so-called grazing angle method [6] is used. In this procedure, the drift of electrons within the sensor is plotted against the production depth (figure 5a) and fitted with a linear function from which the tangent of the Lorentz angle is extracted. The forward pixel modules are slightly rotated about the radial axis of the blades in order to allow charge drift in these modules as well. There, the Lorentz angle is measured with the minimum cluster size method (figure 5b). The goal is to find the minimum of the V-like shape of the average cluster size vs. incidence angle. The cotangent of this angle equals the tangent of the Lorentz angle.

2016 JINST 11 C12057

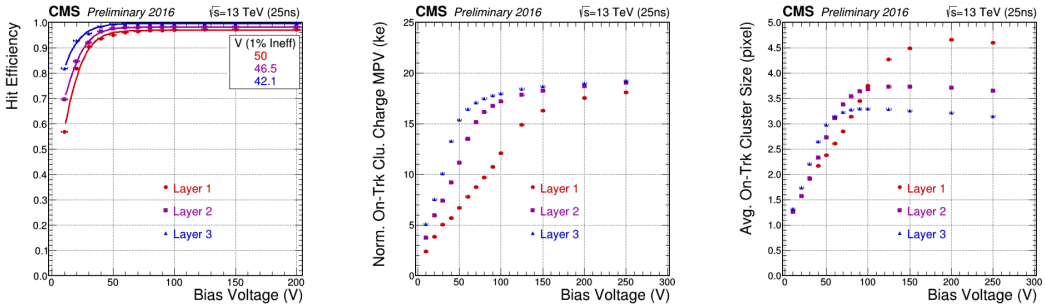

(a) **(b)** **(c)**

Figure 4. a) Hit efficiency, b) MPV of cluster charge and c) average cluster size as a function of high voltage bias for barrel layer modules. In plot a), the hit efficiency points were fitted with a turn-on curve and the top right box indicates the voltage at which the hit efficiency is 1% below the maximum of the function. In plot b) and c), the clusters are attached to tracks. Their charge was corrected for track incidence angle and fitted with a convoluted Landau and Gaussian function. MPV is the most probable value of the function. The scan was taken at the beginning of 2016. The current operation voltage of barrel modules is 200 V.

The measurement in the barrel is shown in figure 6a for various operational temperatures as a function of the applied bias voltage. These measurements are important calibration constants in the offline hit reconstruction. They are monitored since the beginning of the detector's operation (figure 6b). A monotonously increasing trend with accumulated radiation is observed.

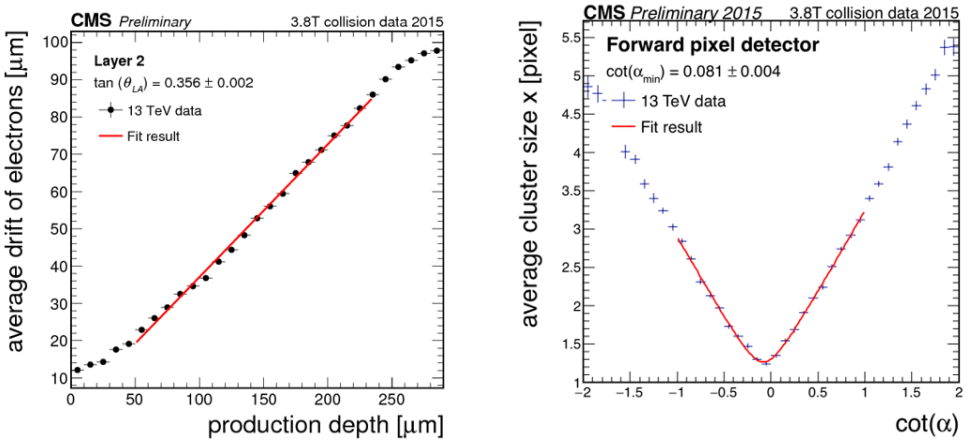

(a) **(b)**

Figure 5. Lorentz angle measurement for a) barrel modules using the grazing angle and b) forward pixel modules using the minimum cluster size method. The local x-direction in the forward modules is approximately the global $r - \phi$ direction (the blades are slightly tilted around the radial direction).

3.2 Pixel thresholds

A general goal is to minimize pixel thresholds in order to maximize the cluster size. For this reason, the average pixel thresholds and noise are important quantities that are monitored throughout the year. The measurement is done by injecting varying amounts of charge to each pixel using an

2016 JINST 11 C12057

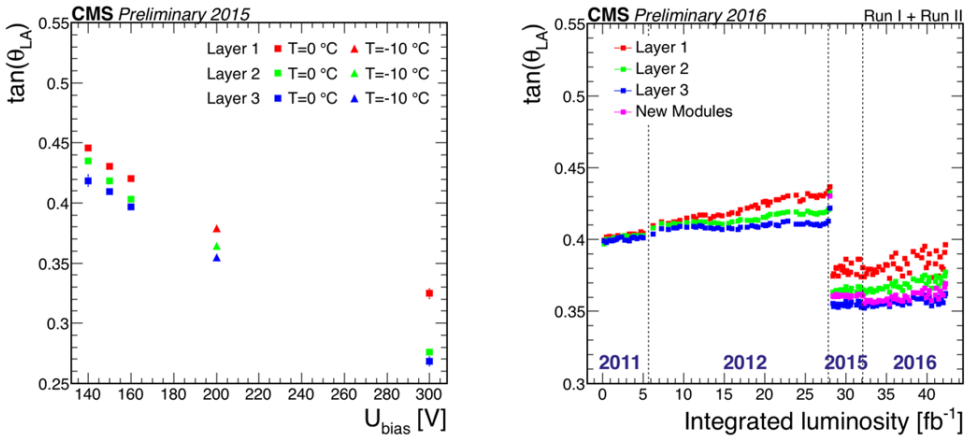

(a) **(b)**

Figure 6. Tangent of the Lorentz angle vs. a) high voltage bias and b) total integrated luminosity (Run I and II combined) for barrel pixel modules. The operation voltage in Run II increased to 200 V, which explains the downward step in 2015 on plot b).

internal circuit and determining the point where the fitted error function reaches 50% efficiency. In 2015, the threshold of new modules rapidly increased with irradiation (figure 7a). A similar trend was observed also in Run I [5]. The noise (figure 7b) quickly reached similar values as that of the old modules, which no longer experience such large changes due to irradiation.

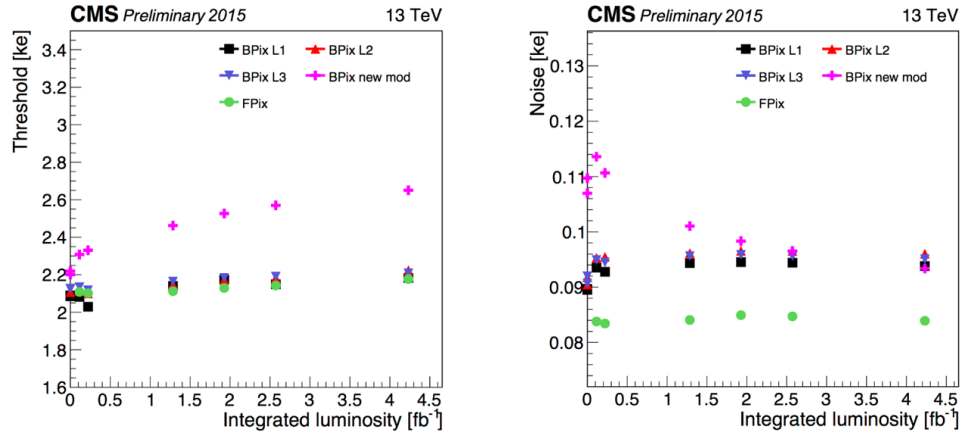

(a) **(b)**

Figure 7. Measured pixel a) threshold and b) noise vs. integrated luminosity in 2015 for new and old modules (the latter are plotted separately for different geometrical locations).

3.3 Cluster properties

Cluster properties like charge and size (figure 8) are important indicators of detector conditions. These are monitored throughout the year. Due to the different levels of irradiation, the old and new modules are calibrated and monitored separately. In the Run I measurements, the MPV

2016 JINST 11 C12057

of the normalized on-track cluster charge changed significantly throughout the year and also after calibrations during technical stop periods (figure 9a). While the MPV of old modules did not change much in 2015 (figure 9b), the new modules showed a rapid increase (figure 9c). This behaviour was also observed for old modules in Run I in the beginning of their lifetime. No significant change in the cluster size (figure 10) was observed.

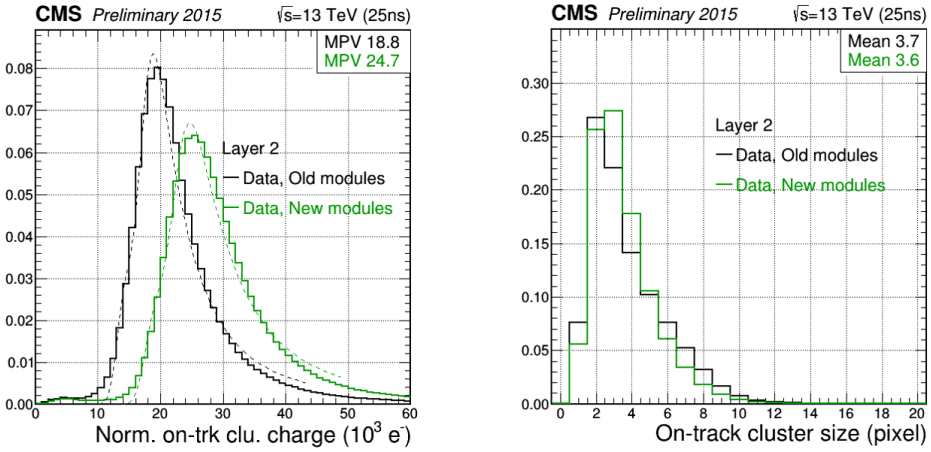

(a) **(b)**

Figure 8. a) Normalized cluster charge and b) cluster size distributions for old and new layer 2 modules. The MPV of convoluted Landau and Gaussians fits and the mean of the distributions are shown in the top right box, respectively.

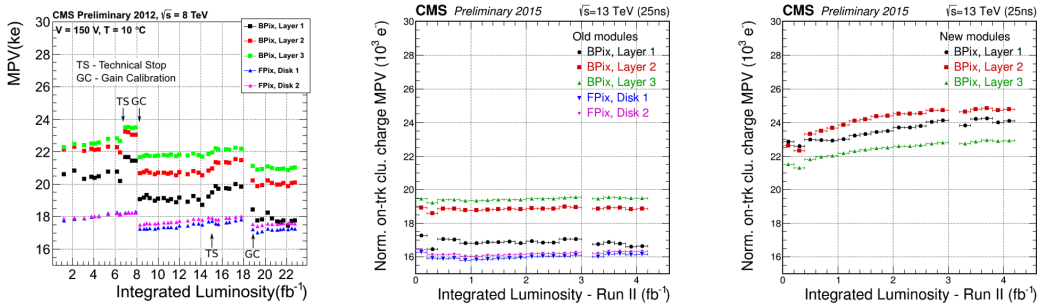

(a) **(b)** **(c)**

Figure 9. The MPV of the normalized on-track cluster charge as a function of integrated luminosity a) in 2012, and in 2015 separately for b) old and c) new modules.

3.4 Hit resolution

Two algorithms are used in CMS for the estimation of the hit positions. One, called the generic algorithm, estimates the hit position based on the charge of the first and last pixel in a cluster. It gives a very fast and relatively accurate hit position estimate (this is used in the high level trigger). The other, called the template algorithm, uses predefined cluster shape templates to find a very accurate hit position. It is based on a detailed simulation (PIXELAV [7]) of the expected pixel

2016 JINST 11 C12057

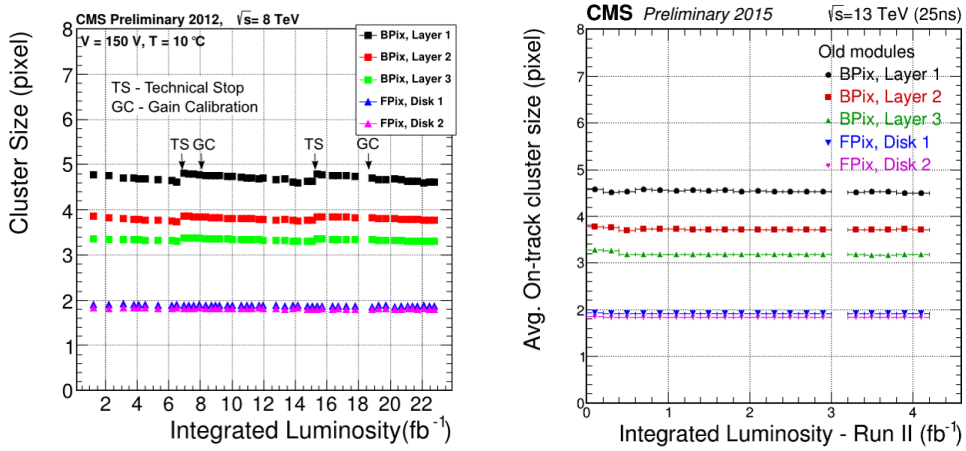

(a) **(b)**

Figure 10. Average on-track cluster size as a function of integrated luminosity in a) Run I and b) Run II. Both old and new modules showed very similar behavior.

cluster shapes in x and y projections for different track incidence angles. PIXELAV also describes radiation damage induced changes. The hit resolution was measured on layer 2 and disk 1 with tracks that have hits on layer 1, and layer 3 or disk 2. The tracks were then re-fitted without the hit in the middle, and the residual between the original and the interpolated hit positions were measured. The residual distribution is then fitted with a student-t function. In order to subtract the effect of the two other layer measurements, the width of the fit is divided by $\sqrt{3/2}$ to get the intrinsic pixel resolution. The template algorithm (which is used in the final fit of the reconstructed tracks) showed superior performance in all cases. A larger improvement was seen in the barrel pixel measurements (figure 11) and a minor one for the forward pixels (figure 12).

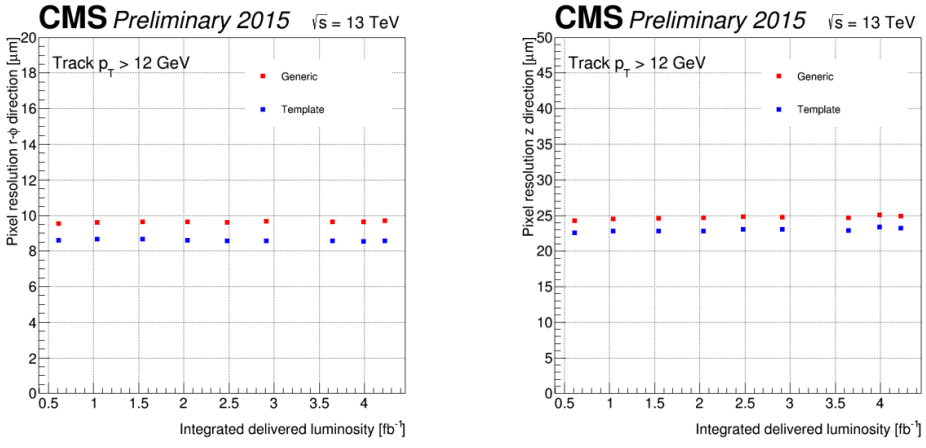

(a) **(b)**

Figure 11. Hit resolution of barrel pixel modules measured with the generic and template reconstruction algorithms in a) the $r-\phi$ and b) the beam direction as a function of integrated luminosity in 2015.

2016 JINST 11 C12057

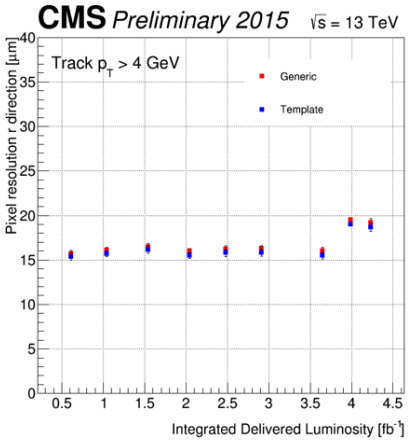

Figure 12. Hit resolution of forward pixel modules measured with the generic and template reconstruction algorithms in the radial direction as a function of integrated luminosity in 2015. The resolution mesurement is seen to depend on the running conditions. In the end-of-year reconstruction, a better alignment was achieved which improved the first seven points significantly.

3.5 Hit efficiency

The hit efficiency (defined in [8]) is also monitored throughout the year. As seen in previous measurements in Run I [9], there is an efficiency loss due to a design limitation of the read-out chips in the current pixel detector. For high instantaneous luminosities, the internal buffer of the readout chips tend to overflow with data, which causes dynamic data losses. The losses are measured in different LHC running conditions. The detector was designed for luminosities up to $10^{34}\,\mathrm{cm}^{-2}\mathrm{s}^{-1}$, which was reached and surpassed later in 2016. The measurements are shown in figure 13. The innermost layer reached inefficiencies of multiple percents, while the other layers and disks showed better performance with efficiencies above 99% in general. The efficiency of layer 1 is shown in figure 14 for various number of colliding bunches in the LHC fills. In order to account for these inefficiencies, double column losses were incorporated in the CMS Simulation [10].

3.6 Single Event Upsets

Single Event Upsets (SEUs) are changes in the state of control registers of the detector caused by ionizing particles. They can degrade or interupt data taking. The typical effect is the disappearance of single pixels (which have a negligible effect) or all clusters in readout chips or larger detector fractions. These intermittent problems are called soft errors, which can be cured by reprogramming the detector. In Run I, several recovery mechanisms were introduced to deal with SEUs [5]. The average rate at which read-out chips turn fully inefficient was recently estimated to be one chip in every $2\,\mathrm{pb}^{-1}$, using measurements in data. A previously introduced recovery mechanism successfully recovered them in cases where a rapid series of errors were detected on a specific channel. Recently an extra automatic recovery mechanism was introduced that fires after reaching a threshold of $50\,\mathrm{pb}^{-1}$ since the last occasion.

2016 JINST 11 C12057

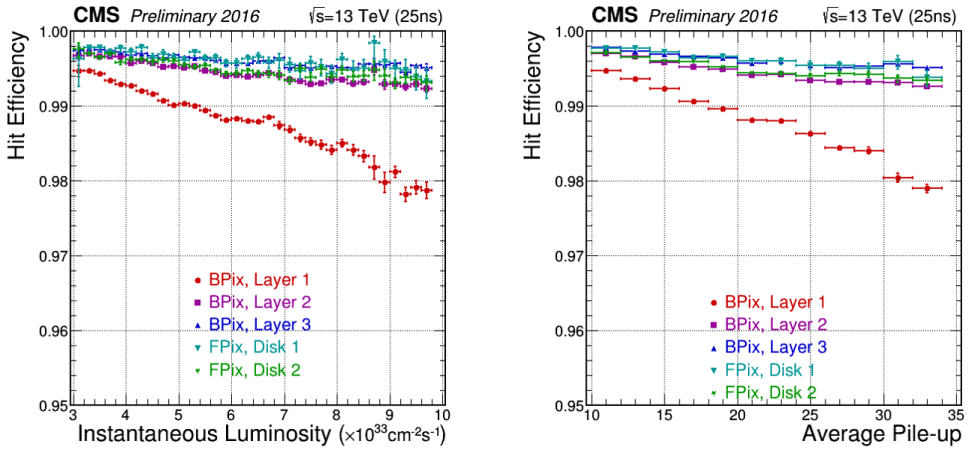

Figure 13. Hit efficiency as a function of a) instantaneous luminosity and b) the average number of inelastic proton-proton collisions (pile-up) in barrel layers and forward disks.

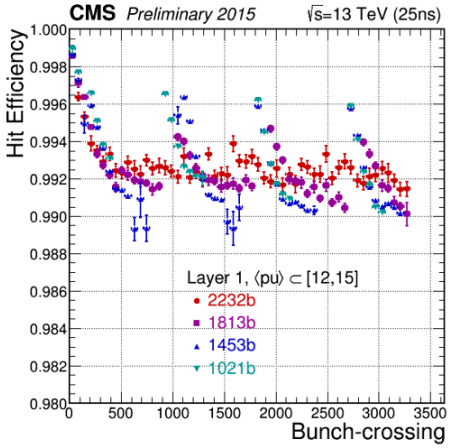

Figure 14. Hit efficiency of the innermost pixel layer as a function of LHC bunch crossing number for different number of colliding bunches in the ring. The average number of inelastic proton-proton collisions (pile-up) was between 12 and 15. The first colliding bunch is preceded by the abort gap (which is comprized of always empty bunches between 3300–3600). After the abort gap, there is enough time for the internal buffers of the readout chip to clear and hence recover full efficiency. For lower number of colliding bunches, there are also smaller gaps between the bunch trains where the efficiency recovers partially.

4 Conclusions

The CMS Pixel detector was successfully commissioned and calibrated after the Long Shutdown 1. During Run II, it showed an overall good performance that matched design expectations. The detector maintained an excellent resolution that initially even surpassed the Run I measurements due to the lowered operational temperature and increased barrel bias voltages. The hit efficiency, was above 99% except for the innermost layer which saw multiple percent losses. In 2017, when the LHC luminosities are expected to increase further, the upcoming upgrade of the detector is

2016 JINST 11 C12057

expected to cure the inefficiency of the current detector. This will enable to maintain and surpass the physics goals of the CMS collaboration.

Acknowledgments

This work is supported by the Hungarian Scientific Research Fund (OTKA K 109803) and the SCOPES 2013-2016 Joint Research Project of the Swiss National Science Foundation.

References

[1] CMS collaboration, *The CMS tracker system project: Technical Design Report*, CERN-LHCC-98-006 (1997) [CMS-TDR-5].

[2] CMS collaboration, *Operational Experience with the CMS Pixel Detector*, 2015 *JINST* **10** C05016 [arXiv:1411.4185].

[3] CMS collaboration, *CMS Technical Design Report for the Pixel Detector Upgrade*, CERN-LHCC-2012-016 [CMS-TDR-11] [FERMILAB-DESIGN-2012-02] [doi:10.2172/1151650].

[4] CMS collaboration, *CMS Pixel status*, *Nucl. Instrum. Meth.* **A 731** (2013) 13.

[5] CMS collaboration, *Radiation experience with the CMS pixel detector*, 2015 *JINST* **10** C04039 [arXiv:1411.5990].

[6] A. Dorokhov et al., *Tests of silicon sensors for the CMS pixel detector*, *Nucl. Instrum. Meth.* **A 530** (2004) 71 [physics/0311050].

[7] M. Swartz, *A Detailed Simulation of the CMS Pixel Sensor*, CERN-CMS-NOTE-2002-027 (2002).

[8] CMS collaboration, *Description and performance of track and primary-vertex reconstruction with the CMS tracker*, 2014 *JINST* **9** P10009 [arXiv:1405.6569].

[9] CMS collaboration, *Operation and performance of the CMS tracker*, 2014 *JINST* **9** C03005 [arXiv:1402.0675].

[10] CMS collaboration, *Simulation of the Dynamic Inefficiency of the CMS Pixel Detector*, 2015 *JINST* **10** C05006 [arXiv:1411.6770].

2016 JINST 11 C12057